Published in final edited form as:
Biochem Pharmacol. 2012 December 1; 84(11): 1419–1427. doi:10.1016/j.bcp.2012.08.020.

1,3-bis(3,5-dichlorophenyl) Urea Compound 'COH-SR4' Inhibits Proliferation and Activates Apoptosis in Melanoma

Sharad S Singhal[1,*], **James Figarola**[1], **Jyotsana Singhal**[1], **Kathryn Leake**[1], **Lokesh Nagaprashantha**[1], **Christopher Lincoln**[2], **B Gabriel Gugiu**[3], **David Horne**[2], **Richard Jove**[2], **Sanjay Awasthi**[1], and **Samuel Rahbar**[1]

[1]Department of Diabetes and Metabolic Diseases Research, Beckman Research Institute, City of Hope, Comprehensive Cancer Center, Duarte, CA 91010

[2]Department of Molecular Medicine, Beckman Research Institute, City of Hope, Comprehensive Cancer Center, Duarte, CA 91010

[3]Department of Mass Spectrometry & Proteomics Core, Beckman Research Institute, City of Hope, Comprehensive Cancer Center, Duarte, CA 91010

Abstract

The current clinical interventions in malignant melanomas are met with poor response to therapy due to dynamic regulation of multiple melanoma signaling pathways consequent to administration of single target agents. In this context of limited response to single target agents, novel candidate molecules capable of effectively inducing tumor inhibition along with targeting multiple critical nodes of melanoma signaling assume translational significance. In this regard, we investigated the anti-cancer effects of a novel dichlorophenyl urea compound called COH-SR4 in melanoma. The SR4 treatment decreased the survival and inhibited the clonogenic potential of melanomas along with inducing apoptosis *in vitro* cultures. SR4 treatments lead to inhibition of GST activity along with causing G2/M phase cell cycle arrest. Oral administration of 4mg/kg SR4 leads to effective inhibition of tumor burdens in both syngeneic and nude mouse models of melanoma. The SR4 treatment was well tolerated and no overt toxicity was observed. The histopathological examination of resected tumor sections revealed decreased blood vessels, decrease in the levels of angiogenesis marker, CD31, and proliferation marker, Ki67, along with an increase in pAMPK levels. Western blot analyses of resected tumor lysates revealed increased PARP cleavage, Bim,

*Address correspondence to: Sharad S. Singhal, Ph.D., Professor, Phone: 626-256-4673, ext 31238; Fax: 626-301-8136; ssinghal@coh.org.

Author's Contributions:
Sharad S. Singhal: Contributed to Research Data and Wrote manuscript
James Figarola: Contributed to Research Data
Jyotsana Singhal: Contributed to Research Data
Kathryn Leake: Contributed to Research Data
Lokesh Nagaprashantha: Contributed to Research Data
Christopher Lincoln: Contributed to Research Data
Gabriel Gugiu: Contributed to Research Data
David Horne: Contributed to Review/edit manuscript
Richard Jove: Contributed to Review/edit manuscript
Sanjay Awasthi: Contributed to Discussion and Review/edit manuscript
Samuel Rahbar: Contributed to Discussion and Review/edit manuscript

pAMPK along with decreased pAkt, vimentin, fibronectin, CDK4 and cyclin B1. Thus, SR4 represents a novel candidate for the further development of mono and combinatorial therapies to effectively target aggressive and therapeutically refractory melanomas.

Keywords

Melanoma; SR4; syngeneic model; tumor xenografts

1. Introduction

Melanoma arises from the malignant transformation of the pigmented cells of the skin called melanocytes. The incidence of cutaneous melanoma has been rising in the past decade. Melanoma represents only 4% of all skin cancers, but causes nearly 80% of skin cancer related deaths [1]. Melanoma has a positively skewed risk towards fair skinned and young individuals [2]. Metastatic melanoma is an almost certain death sentence because of the highly refractory nature of this malignancy [3]. The transformation of normal melanocytes in to melanoma cells is initiated by a complex spectrum of interacting genetic and environmental factors, some of them having the potential to trigger oncogenic cascade alone. The established risk factors for melanoma include exposure to UVB rays [4]. The UVB activates growth factor phosphorylation to enhance mitogenic signaling in transforming melanoma cells [5].

The cellular inputs that reprogram melanoma signaling are modulated by a complex set of cytoplasmic and nuclear networks. Metastatic melanoma remains a daunting therapeutic challenge because of simultaneous dysregulation of multiple important signaling pathways that suppress apoptosis and promote growth and invasion [6]. A Majority of the patients with metastatic melanoma with refractoriness to therapy have $V^{600}E$ mutations in BRAF which leads to continuous activation of the MAPK pathway [7, 8]. BRAF targeted therapy has recently emerged as the most effective therapy for melanoma, but response rates are less than desirable and survival advantage is relatively short [9]. Melanoma is a cell type typically very rich in mercapturic acid pathway enzymes like glutathione S transferases (GSTs) which play a vital role in the survival, apoptosis and drug-sensitivity of melanomas [10].

Currently there are no effective chemotherapeutic strategies that are safe, affordable and effective given the limited treatment options available for advanced stages of melanoma [11]. Hence, the development of novel targeted therapy assumes immense translational significance in contemporary melanoma research. Based on our screening to identify novel products with anti-cancer activities we have identified the anti-cancer effects of a dichlorophenyl urea compound called “COH-SR4” in various cancers. SR4 is 1,3-bis(3,5-dichlorophenyl)urea, which has shown promising anti-cancer activity against human leukemia cells [12]. In this study, following initial *in vitro* studies in melanoma cultures, we studied the anti-cancer effects and the respective mechanisms of action of SR4 in syngeneic and transgenic mouse models of melanoma.

2. Materials and Methods

2.1. Reagents

Terminal deoxynucleotidyl-transferase deoxyuridine triphosphate nick-end labeling (TUNEL) fluorescence and avidin/biotin complex (ABC) detection kits were purchased from Promega (Madison, WI) and Vector (Burlingame, CA), respectively. MTT, Horseradish peroxidase (HRP)-conjugated anti-mouse, and anti-rabbit secondary antibodies

were procured from Sigma (St. Louis, MO). PARP, β-actin, fibronectin, vimentin, Bim, Bcl2, cyclin B1, CDK4, Akt, pAkt (S^{473}), GAPDH, Ki67, CD31 and pAMPK (T^{172}) antibodies were purchased from Santa Cruz Biotechnology (Columbus, OH) and Cell Signaling Technologies (Danvers, MA). GSTπ siRNA (GSTP1_1 FlexiTube siRNA; SI00300349) was purchased from Qiagen (Valencia, CA)

2.2. Synthesis of SR4

The 1,3-bis(3,5-dichlorophenyl)urea compound SR4 ($C_{13}H_8Cl_4N_2O$, MW = 350.03) was synthesized according to a previously validated protocol by Dr. Christopher Lincoln, Director of Chemical GMP Synthesis Facility, Beckman Research Institute, City of Hope National Medical Center, Duarte, CA [12] . Briefly, 3,5-dichlorophenyl isocyanate (1.21g (96%), 6.17 mmol) was added portion-wise to a stirring solution of 3,5-dichloroaniline (1.00g (98%), 6.33 mol) in dichloromethane (15 mL) under N_2. After 19 h at ambient temperature, the entire reaction mixture was filtered and the filter cake was washed with dichloromethane (2 × 10 mL). The solid was dried *in vacuo* to afford 1,3-bis(3,5-dichlorophenyl)urea (1.78g, 82%) as a white crystalline solid. ^{1}H-NMR (400 MHz, DMSO-d6) δ 9.35 (s, 2H), 7.53 (d, J = 1.8 Hz, 4H), 7.17 (t, J = 1.8 Hz, 3H); ^{13}C NMR (100 MHz, DMSO-d6) δ 152.0, 141.8, 134.1, 121.3, 116.7; HRMS-ESI (m/z (%)) 348.9278 (100), 346.9310 (73), 350.9255 (48), 349.9323 (10), 352.9239 (8), 347.9357 (7), 351.9303 (4).

2.3. Cell Lines and Cultures

Mouse (B16-F0) and human (A2058 and Hs600T) melanoma cell lines were purchased from the American Type Culture Collection (ATCC, Manassas, VA) in October 2011. Normal human aortic vascular smooth muscle cells (HAVSMC) were kindly authenticated and donated by Dr. Paul Boor, University of Texas Medical Branch, Galveston, TX. All cells were cultured at 37 °C in a humidified atmosphere of 5 % CO_2 in the appropriate medium: RPMI-1640 (A2058) and DMEM (HAVSMC, B16-F0 and Hs600T) medium supplemented with 10 % heat-inactivated FBS and 1% penicillin/streptomycin (P/S) solution. All the cells were also tested for *Mycoplasma* once every 3 months.

2.4. siRNA mediated knock-down of GSTπ

Cells were transfected with scrambled and GSTπ siRNA at the concentration of 10 μg / ml in serum free medium, using Lipofectamine 2000 (Invitrogen, Carlsbad, CA) for 3 h, according to the manufacturer's instructions. Excess siRNA was washed off with PBS and complete medium (i.e. with FBS) was added. After 24 h silencing, cells were exposed with SR4. After 96 h incubation, MTT assays as well as Western blot analyses for GSTπ expression were performed.

2.5. Cell survival (MTT) assay

Cell density measurements were performed using a hemocytometer to count reproductive cells resistant to staining with trypan blue. Approximately 20,000 cells were plated into each well of 96-well flat-bottomed micro-titer plates. After 12 h incubation at 37 °C, medium containing SR4 (ranging 0–200 μM) were added to the cells. After 96 h incubation, 20 μl of 5 mg/ml MTT were introduced to each well and incubated for 2 h. The plates were centrifuged and medium was decanted. Cells were subsequently dissolved in 100 μl dimethyl-sulfoxide with gentle shaking for 2 h at room temperature, followed by measurement of optical density at 570 nm [13].

2.6. TUNEL Apoptosis assay

For TUNEL assay,1×10^5 cells were grown on the cover slips for ~12 h followed by treatment with SR4 (10 μM) for 24 h. Apoptosis was determined by the labeling of DNA

fragments with terminal deoxynucleotidyl-transferase dUTP nick-end labeling (TUNEL) assay using Promega fluorescence apoptosis detection system according to the protocol described previously [14, 15].

2.7. Flow cytometry analysis of cell cycle regulation

2×10^5 cells were treated with SR4 (10 μM) for 18 h at 37 °C. After treatment, floating and adherent cells were collected, washed with PBS, and fixed with 70 % ethanol. On the day of flow analysis, cell suspensions were centrifuged; counted and same numbers of cells were resuspended in 500 μl PBS in flow cytometry tubes. Cells were then incubated with 2.5 μl of RNase (stock 20 mg/ml) at 37 °C for 30 min after which they were treated with 10 μl of propidium iodide (stock 1mg/ml) solution and then incubated at room temperature for 30 min in the dark. The stained cells were analyzed using the Beckman Coulter Cytomics FC500, Flow Cytometry Analyzer. Results were processed using CXP2.2 analysis software from Beckman Coulter.

2.8. Analysis of SR4 in serum by Mass Spectrometry

Mice (n=3 each for control and SR4 treatment) were administered either 0.2 ml corn oil or 100 μg SR4 /0.2 ml corn oil/mice (4 mg/kg b.w.) by oral gavage on alternate days for 8 weeks. On the last day, the blood was collected within 2 h after final dosage. To 50 μL serum was added 0.5 μL 5 μg/uL 6D-SR4 standard in DMSO and 500 uL ethyl acetate. The samples were vortexed for 1 min and then spun down in a bench-top centrifuge for 2 min. Then 400 μL of the organic layer was collected, evaporated to dryness and redisolved in 500 uL methanol for analysis. After an initial concentration test, 50 μL were taken and diluted to 2 mL with methanol for final analysis. A calibration curve was built using a serial dilution of SR4 (from 0.1pg/uL to 1 ng/uL) in 125 pg/μL 6D-SR4.

SR4 and 6D-SR4 were separated by HPLC using an Agilent Zorbax 0.5×150mm C18, 5um column with a flow rate of 50 μL/min and a gradient of 65% B to 95% B over 4 min, then 2 min at 95%B and 1 min back to 65%B. Buffer A was 5mM ammonium formate and buffer B was 5 mM ammonium formate in methanol. The elute from the column was introduced into an Agilent 6410 triple quadrupole tandem mass spectrometer by electrospray ionization (ESI) through a capillary maintained at 4kV, using 6L/min nitrogen nebulizing gas at 350 °C and 15 psi, fragmentor voltage = 190V. The following transitions were monitored in positive ion mode: 344 > 127.1 and 355 > 130.1(collision energy = 28V), 344 > 161.9 and 355 >164.9 (C.E.= 20V) for SR4 and 6dSR4. Quantitation was achieved using Masshunter Quantitative Analysis 5(Agilent Technologies) using a linear calibration curve.

2.9. In vivo xenograft studies

C57B mice (for syngeneic B16-F0 mouse melanoma model) and Hsd: Athymic nude nu/nu mice (for A2058 human melanoma mouse xenografts model), were obtained from Harlan, Indianapolis, IN. All animal experiments were carried out in accordance with a protocol approved by the Institutional Animal Care and Use Committee (IACUC). In each model, ten 10-weeks-old mice were divided into two groups of 5 animals (treated with corn oil (vehicle), and SR4 compound 4 mg / kg b.w.). All animals were injected with 2×10^6 melanoma cells suspensions in 100 μl of PBS, subcutaneously into one flank of each mouse. At the same time, animals were randomized into treatment groups as indicated in the figures (Supplementary Figs 2 and 3). Treatment was started 10 days after the implantation to see palpable tumor growth. Treatment consisted of 0.1 mg of SR4/mice in 200 μl corn oil by oral gavage alternate day. Control groups were treated with 200 μl corn oil by oral gavage alternate days. Animals were examined daily for signs of tumor growth. Tumors were measured in two dimensions using calipers. Photographs of animals were taken at day 1, day 10, day 14, day 18, day 20, day 30, and day 51 after subcutaneous injection, are shown for

all groups. Photographs of tumors were also taken at day 20 (for syngeneic model), and at day 51 (for xenograft model).

2.10. Histopathological examination of tumors for angiogenic, proliferative and differentiation markers

Control and SR4 treated B16-F0 and A2058 melanoma bearing mice tumor sections were used for histopathologic analyses. Immuno-histochemistry analyses were performed for Ki-67 expression (marker of cellular proliferation), CD31 (angiogenesis marker), and pAMPK (cellular regulator of lipid and glucose metabolism) from tumors in mice of control and SR4-treated groups. Statistical significance of difference was determined by two-tailed Student's t test. $p < 0.001$, SR4-treated compared with control. Immuno-reactivity is evident as a dark brown stain, whereas non-reactive areas display only the background color. Sections were counterstained with Hematoxylin (blue). Photomicrographs at 40× magnification were acquired using Olympus DP 72 microscope. Percent staining was determined by measuring positive immuno-reactivity per unit area. Arrows represent the area for positive staining for an antigen. The intensity of antigen staining was quantified by digital image analysis using DP2-BSW software. Bars represent mean ± S.E. (n = 5); * $p<0.001$ compared with control.

2.11. Statistical Analyses

All data were evaluated with a two-tailed unpaired student's t test and are expressed as the mean ± SD. The statistical significance of differences between control and treatment groups was determined by ANOVA followed by multiple comparison tests. Changes in tumor size and body weight during the course of the experiments were visualized by scatter plot. Differences were considered statistically significant when the *p* value was less than 0.05.

3. Results

3.1. Anti-proliferative and pro-apoptotic effect of SR4 in Melanoma

The dichlorophenyl urea compound SR4 was synthesized by the Drug Discovery Core Facility within City of Hope's Comprehensive Cancer Center [12]. The structure of SR4 is represented in Figure 1 (**panel A**). The extent of melanoma cell survival was analyzed by MTT assay following treatment with SR4 for 96 h. The SR4 treatment had a strong inhibitory effect on the survival of melanoma cells [IC_{50}: B16-F0 cell line-5 ± 1 μM, Hs600T cell line-6 ± 1 μM, and A2058 cell line-11 ± 2 μM]. SR4 did not cause any significant cytotoxicity in normal human aortic vascular smooth muscle cells (HAVSMC) (Fig 1B). The anti-proliferative effects of SR4 were further examined by colony forming assay. The SR4 (10 μM) treatment resulted in 38 ± 9 %, 48 ± 5 % and 37 ±4% colony formation in B16-F0, Hs600T and A2058 melanoma cells. The SR4 treatment did not significantly affect the colony forming ability of HAVSMC as the HAVSMC cells displayed 96 ± 4% colony forming potential compared to respective untreated controls (Fig 1C). The 10 μM of SR4 treatment for 24 h induced apoptosis in B16-F0 and A2058 melanoma cells as determined by enhanced DNA fragmentation in TUNEL apoptotic assay (Fig 1D). The cytotoxicity of SR4 in melanoma cells as evident by MTT, clonogenic survival and apoptotic assays revealed that SR4 is a potential lead compound for melanoma. Also, independent cytotoxicity testing from the NCI-60 DTP Human Tumor Cell Line Screen further confirmed the potential anti-cancer activities of SR4 against several melanoma cell lines (Supplementary Figure 1).

3.2. Effect of SR4 on GST activity in melanoma cells

GSTs are a class of phase II detoxifying enzymes, which mediate drug resistance by detoxifying administered chemotherapy drugs for efflux out of cells by transport proteins. The over-expression of GSTs is associated with malignant progression of many cancers including melanoma, lung and prostate cancers [10, 16, 17]. GSTs mediate glutathione conjugation of toxic end products of lipid peroxidation like 4-hydroxy-2-nonenal (4-HNE) which eventually leads to buffering of tumor-toxic oxidative stress and favors tumor survival and proliferation in hypoxic environment [18]. Hence, we investigated the effect of SR4 on the enzymatic activity of GSTs towards 1-chloro 2,4-dinitro benzene (CDNB), a model substrate routinely used for GST activity [19]. The SR4 treatment inhibited the total GST activity to a significant extent in the B16-F0, Hs600T and A2058 melanoma cells (Fig 2A). The ability of SR4 to inhibit GST activity in melanomas represents a potential mechanism that contributes to decreased survival of melanoma cells following SR4 treatment (Fig 2A).

3.3. GSTπ depletion is associated with cytotoxicity in melanoma cells

SR4 treatment significantly decreased the GST activity in both mouse and human melanomas cells (Fig 2A). Given the significant role of GSTπ in tumor progression (17), we further studied the impact of knock-down of GSTπ by transfection using GSTP1-1 siRNA in B16-F0, Hs600T and A2058 melanoma cells. The knock-down of GSTπ was confirmed by Western-blot analyses (Fig 2B). The MTT assay revealed that GSTπ-depletion itself decreased cell growth by ~35–46 % (Fig 2C inset), and sensitized to SR4 significantly by decreasing the IC_{50} to almost half (Fig 2C). Taken together, these studies suggest that SR4 targets GSTπ activity and that GSTπ inhibition further sensitizes to the growth inhibitory effects of SR4 in melanoma. The anti-proliferative effect of SR4 was further examined by cell cycle FACS analysis. SR4 treatment caused G2/M phase arrest in both B16-F0 mouse and A2058 human melanoma cells (~50% cells accumulated in G2 phase) (Fig 2D).

3.4. Analyses of SR4 in mice serum

Next, we assessed the absorption of orally administered SR4 in mice. The C57 B mice were treated with 0.1 mg/mice (4 mg/kg b.w.) of SR4 on alternate day for 8 weeks. The blood was collected within 2h of the dosing on the final day of treatment and further processed for MS analyses as described in the methods section. LC-MS/MS analysis of SR4 treated mice serum revealed that SR4 is effectively absorbed after oral dosage and it reaches a serum concentration of 342 ± 44 μg/L (equivalent to 1± 0.22 μM) (Fig 3A–D).

3.5. Analyses of blood chemistries in control and SR4 treated mice

To evaluate the potential toxicity of SR4 on animals, C57 B mice were treated with 0.1 mg/mice (4 mg/kg b.w.) of SR4 or with vehicle on alternate day for 2 weeks (n = 6). After the treatment period, blood and plasma/serum were isolated and analyzed. Oral administration of SR4 showed no significant differences on key blood and metabolic profiles as compared with vehicle-treated mice. The plasma alanine transaminase (ALT) and alkaline phosphatase (ALP) were moderately higher in SR4-treated mice ($p < 0.05$), while the levels of two other liver enzymes; aspartate transaminase (AST) and lactate dehydrogenase (LDH) were similar with control mice (Supplementary Table 1).

3.6. Anti-neoplastic effect of SR4 in vivo on melanoma progression

C57B mice (for syngeneic B16-F0 mouse melanoma model) and Hsd: Athymic nude nu/nu mice (for A2058 human melanoma mouse xenografts model), were used for testing the impact of oral administration of SR4 on melanoma progression *in vivo* models. In each model, ten 10-weeks-old mice were divided into two groups of 5 animals (treated with corn

oil (vehicle), and SR4 compound (4 mg / kg b.w.). All animals were injected with 2 × 10^6melanoma cells suspensions in 100 μl of PBS, subcutaneously into one flank of each mouse. Treatment was started 10 days after the implantation of melanoma cells. Treatment consisted of 0.1 mg of SR4/mice in 200 μl corn oil by oral gavage on alternate days. Control groups were treated with 200 μl corn oil by oral gavage alternate day. In our studies, the SR4 treatment was tolerated well by the mice without any weight loss compared with age-matched controls (Fig 4A). Animals were examined daily for signs of tumor growth. Tumors were measured in two dimensions using calipers. The SR4 treatment lead to significant reduction in the tumor burdens in the treated groups [B16-F0 syngeneic melanoma model: 2.36 ± 0.2 g *vs.* 1.07 ± 0.2 g in control and SR4 treated groups, respectively on day 20. A2058 human melanoma xenograft model: 1.91 ± 0.3g *vs.* 0.7 ± 0.1 g in control and treated and groups, respectively, on day 51] (Fig 4B). Photographs of animals were taken at day 1, day 10, day 14, day 18, day 20, day 30 and day 51 after subcutaneous injection, are shown for all groups. Photographs of tumors were also taken at day 20 (for syngeneic model), and at day 51 (for xenograft model) (Supplementary Figs 2 and 3). The time course analyses of SR4 treatment revealed a substantial inhibition of tumor progression in both syngeneic and xenografts models of melanoma whereas uncontrolled growth was observed in untreated controls (Figure 4C). In parallel xenografts studies, we also used 20 mg / kg b.w. SR4 to see the better regression and any toxicity. Higher dosage of SR4 caused no further improvement in tumor regression and no toxicity was observed (Supplementary Fig 3). The SR4 treated animals with B16 melanoma survived for 50 ± 5 days, while all animals treated with vehicle only were censored by day 20 ± 2. The SR4 treated animals with A2058 melanoma were still alive at 88 days, while all animals treated with vehicle only were censored by day 51 ± 3. These results indicated that SR4 administration inhibits melanoma growth and prolongs survival without causing side effects.

3.7. Impact of SR4 on the markers of proliferation and angiogenesis

Following the *in vivo* animal studies, the histopathological examination of paraffin-embedded tumor xenograft sections by H&E staining revealed that SR4 reduces the number of tumor blood vessels and restores the normal morphology when compared to controls (Fig 5). SR4 treatment decreased the levels of proliferation marker, Ki 67 and angiogenesis marker, CD31 as revealed by ABC staining. AMPK is a critical cellular protein which senses the low energy status of cells and inhibits proliferation and survival of cells [20]. SR4 treatments lead to increase in the levels of pAMPK in tumor sections which provides corroborative evidence for the induction of anti-tumor effects in *in vivo* models of melanoma.

3.8. Effect of SR4 on the expression of tumor proteins

The SR4 treated groups had high levels of the cleaved PARP compared to untreated controls, which is in accordance with the observed apoptotic effects of SR4 *in vitro* melanoma cultures. Akt is a critical signaling protein that transduces the proliferative signals from upstream integrins and growth factor receptors [21]. The SR4 treatments lead to an increase in the levels of PARP cleavage along with decrease in the levels of Akt and pAkt (S^{473}). The cellular levels of vimentin and fibronectin determine the extent of migration and proliferation in melanoma cells [22, 23]. SR4 treatments lead to decreases in the expression of vimentin and fibronectin which are associated with invasive progression of melanomas. SR4 treated groups had an enhanced expression of pro-apoptotic protein Bim along with a parallel decrease in the levels of anti-apoptotic protein Bcl2. The expression of cell cycle regulatory proteins CDK4 and Cyclin B1 was decreased following SR4 treatment. Our results regarding G2/M phase arrest was observed consequent to SR4 treatment are in accordance with some of the published studies which indicate that that anti-cancer compounds such as apigenin and thimerosal which also cause inhibition of CDK4 along

with cyclin B1 [24, 25]. In accordance with the histopathological examination, the levels of pAMPK (T^{172}) were enhanced in SR4 treated groups compared to controls in both B16-F0 and A2058 melanoma (Fig 6).

4. Discussion

The development of novel interventional strategies and effective chemotherapies for melanomas remains one of the frontier challenges in clinical oncology, given the fact that melanoma is one of the top ten cancers with an increasing risk on incidence in Caucasian populations. The current therapeutic options for melanomas are limited. The drugs used in melanoma therapy include temozolomide, dacarbazine, hydroxyureas and interleukin-2 along with the recent approval of vemurafenib for advanced and metastatic melanomas over-expressing BRAF $V^{600}E$ mutation [26]. However, the response to chemotherapy is limited and resistance is prominent in many cases of melanomas as reported by several studies [27, 28]. Thus, new molecules capable of being effective in inducing anti-tumor effects along with regulatory effects on tumor signaling proteins of specific significance in melanoma progression and therapeutic resistance present as significant candidates for further stages of clinical drug development. In this regard, the results from our investigations on the anti-cancer effects and mechanisms of action of SR4 assume significance.

The efficacy of radiotherapy relies on the oxidative stress induced generation of hydroxyl radicals and consequent DNA damage. The oxidative stress induced due to radiotherapy also enhances the generation of cellular levels of lipid peroxidation products which contribute to the toxic effects of radiotherapy [15]. The products of lipid peroxidation like 4-hydroxy-nonenal (4-HNE) and chemotherapy drugs, are rapidly conjugated to glutathione (GSH) by intracellular GSTs to form GSH adducts (electrophilic-conjugates or GS-E). The formation of GS-E is a rate limiting step in the process of detoxification of toxic products of lipid peroxidation [29]. As, the expression of GSTs is increased in malignant melanoma, the inhibition of GST activity by SR4 is a significant finding for further studies on SR4 towards possibly potentiating the effects of radiotherapy and chemotherapy. SR4 treatment effectively induced the cell cycle arrest in melanoma cells. The oral administration of SR4 was well tolerated without any overt toxicity along with inducing effective tumor inhibition in both syngeneic and xenografts mouse models of melanoma.

Our studies indicate that SR4 is tolerable and effective anti-cancer agent with no overt toxicity *in vivo* models of melanoma. One of the members of this class of compounds namely 1,3-bis (3,4-dichlorophenyl) urea, a close relative of SR4, was studied earlier by Proctor et al. as compound II, was demonstrated to be an electron transport inhibitor that reduced Staphylococcus aureus hemolytic activity and to protected cultured endothelial cells from lysis [30]. In their studies on compound II, they found that the effective dose for the inhibition of bacterial respiration was 50 times lower than the concentration required to cause similar inhibition of rat mitochondrial respiration and also human and animal exposure studies showed a lack of acute toxic responses to compound II.

The analyses of the expression of tumor proteins consequent to SR4 treatment revealed the impact on significant nodes of melanoma proliferation, invasion and metastases. In melanomas, the tumor growth phases include “radial growth phase (RGP)” and“vertical growth phase (VGP)”. Melanomas behave as highly metastatic tumors after invading the dermis and hence, malignant melanomas in RGP are usually surgically excised but post-surgical recurrence is common from satellite lesions, which become aggressive once the primary tumor is removed [31]. Thus, the tumor proteins which regulate the transition from RGP to VGP in melanoma hold significant promise in developing targeted therapies. In a study, reverse phase protein array analyses of resected melanoma tissues revealed that the

expression levels of Akt is high in advanced and metastatic melanomas [32]. The over-expression of Akt leads to conversion of RGP to VGP in melanoma [33]. Akt activation is known to mediate resistance to microtubule targeting agents as well as BRAF and MEK inhibitor AZD6244 or Vemurafenib [34, 35]. Thus, the inhibition of Akt phosphorylation by SR4 represents an interesting finding for targeting the progression and drug-resistance in melanomas.

The Bcl2 family proteins play a vital role in the survival and apoptosis of various cancers including melanoma [36]. The anti-apoptotic protein Bcl-2 is a natural and preferred target that needs to be inhibited for successful melanoma interventions. Among the human epidermal cells, melanocytes are the only cells that constitutively express Bcl2 and the Bcl2 expression is enhanced with malignant transformation [37, 38]. Also, Bcl-2 knockout mice display rapid greying of hair because of decreased survival of follicular melanocytes [39]. Elevated levels of Bcl2 are associated with enhanced survival and chemotherapy resistance in melanoma. The expression of pro-apoptotic protein Bim, a protein known to antagonize the functions of Bcl2, is decreased in cutaneous melanomas and this is associated with poor 5-year survival [40]. Thus, the decreased expression of anti-apoptotic Bcl-2 and increased expression of pro-apoptotic Bim reinforce the relevance of mechanisms of action of SR4 in causing apoptosis in melanoma.

The inhibition of the expression of cell cycle regulatory proteins cyclin B1 and CDK4 provides corroborative rationale for the impact of SR4 on cell cycle progression in melanoma. The inhibition of cyclin B1 is also associated with response to gamma-irradiation therapy which, along with the inhibition of GST activity by SR4, provides rationale for further combinatorial studies with radiotherapy [41]. The epithelial mesenchymal transformation (EMT) during the transformation and metastasis leads to expression of transcription factors like snail and slug, which in turn enhance the expression of fibronectin and vimentin [42]. The proliferating and invading melanoma cells express a variant of fibronectin which can be rapidly secreted out of cells and can activate haptotactic migration of melanoma cells [43]. The over-expression of vimentin in a weakly invasive A 375P melanoma cell line lead to a two-to three fold increase in the invasion through basement membrane matrix as well as migration *in vitro* [23]. The over-expression of vimentin is also associated with hematogenous metastases of melanoma cells [44]. Thus, the inhibition of fibronectin and vimentin by SR4 assumes translational significance.

The AMPK signaling regulates vital processes of proliferation and survival in many cancers. AMPK is activated by high levels of AMP/ATP ratio or decreased cellular energy status which leads to decreased metabolic activity and proliferation consequent to AMPK activation in energy deficient cells [45]. Cancer cells suppress the activation of AMPK in spite of imbalance between cellular energy *vs.* rate of proliferation and thus sustain active growth and invasion [20]. The BRAF $V^{600}E$ mutations lead to constitutive inhibition of AMPK (T^{172}) phosphorylating kinase LKB1, which results in low levels of AMPK activation in melanoma cells [46]. Thus, the enhanced phosphorylation of AMPK (T^{172}) by SR4 as revealed by both histopathological analyses of resected tumor sections (Fig 5) and Western blot analyses of tumor tissue lysates following SR4 treatment is another significant mechanistic finding in the context of melanoma pathogenesis and progression (Fig 6).

In summary, the increasing incidence of melanomas along with high rates of therapeutic refractoriness to conventional modes of clinical interventions necessitate characterization and validation of novel anti-cancer compounds for mono and combinatorial therapy in melanomas. In this regard, the inhibitory effects and mechanisms of action of SR4 as validated by both syngeneic and transgenic mouse models of melanoma provide strong and relevant mechanistic rationale for further translational studies.

Supplementary Material

Refer to Web version on PubMed Central for supplementary material.

Acknowledgments

This work was supported in part by USPHS grant CA 77495 (to SA) and CA 115674 (to RJ).

The abbreviations used are

COH-SR4 1,3-bis(3,5-dichlorophenyl)urea “City of Hope compound”

References

1. Linos E, Swetter SM, Cockburn MG, Colditz GA, Clarke CA. Increasing burden of melanoma in the United States. J Invest Dermatol. 2009; 129:1666–74. [PubMed: 19131946]
2. MacKie RM. Incidence, risk factors and prevention of melanoma. Eur J Cancer. 1998; 34:S3–6. [PubMed: 9849401]
3. Albert VA, Koh HK, Geller AC, Miller DR, Prout MN, Lew RA. Years of potential life lost: Another indicator of the impact of cutaneous malignant melanoma on society. J Am Acad Dermatol. 1990; 23:308–10. [PubMed: 2212128]
4. Lea CS, Scotto JA, Buffler PA, Fine J, Barnhill RL, Berwick M. Ambient UVB and melanoma risk in the United States: A case-control analysis. Ann Epidemiol. 2007; 17:447–53. [PubMed: 17395487]
5. Huang RP, Wu JX, Fan Y, Adamson ED. UV activates growth factor receptors via reactive oxygen intermediates. J Cell Biol. 1996; 133:211–20. [PubMed: 8601609]
6. Gray-Schopfer V, Wellbrock C, Marais R. Melanoma biology and new targeted therapy. Nature. 2007; 445:851–7. [PubMed: 17314971]
7. Solit DB, Garraway LA, Pratilas CA, et al. BRAF mutation predicts sensitivity to MEK inhibition. Nature. 2006; 439:358–62. [PubMed: 16273091]
8. Smalley KS, Flaherty KT. Integrating BRAF/MEK inhibitors into combination therapy for melanoma. Br J Cancer. 2009; 100:431–5. [PubMed: 19156138]
9. Emery CM, Vijayendran KG, Zipser MC, et al. MEK1 mutations confer resistance to MEK and BRAF inhibition. Proc Natl Acad Sci U S A. 2009; 106:20411–6. [PubMed: 19915144]
10. Moral A, Palou J, Lafuente A, et al. Immunohistochemical study of alpha, mu and pi class glutathione S transferase expression in malignant melanoma. MMM group. Multidisciplinary malignant melanoma group. Br J Dermatol. 1997; 136:345–50. [PubMed: 9115913]
11. Woodman SE, Lazar AJ, Aldape KD, Davies MA. New strategies in melanoma: Molecular testing in advanced disease. Clin Cancer Res. 2012; 18:1195–200. [PubMed: 22275506]
12. Figarola JL, Weng Y, Lincoln C, Horne D, Rahbar S. Novel dichlorophenyl urea compounds inhibit proliferation of human leukemia HL-60 cells by inducing cell cycle arrest, differentiation and apoptosis. Invest New Drugs. 2012; 30:1413–25. [PubMed: 21728022]
13. Singhal SS, Sehrawat A, Sahu M, et al. RLIP76 transports sunitinib and sorafenib and mediates drug resistance in kidney cancer. Int J Cancer. 2010; 126:1327–38. [PubMed: 19626587]
14. Singhal SS, Yadav S, Drake K, Singhal J, Awasthi S. Hsf-1 and POB1 induce drug sensitivity and apoptosis by inhibiting Ralbp1. J Biol Chem. 2008; 283:19714–29. [PubMed: 18474607]
15. Singhal J, Singhal SS, Yadav S, et al. RLIP76 in defense of radiation poisoning. Int J Radiat Oncol Biol Phys. 2008; 72:553–61. [PubMed: 18793957]
16. Ritchie KJ, Henderson CJ, Wang XJ, et al. Glutathione transferase pi plays a critical role in the development of lung carcinogenesis following exposure to tobacco-related carcinogens and urethane. Cancer Res. 2007; 67:9248–57. [PubMed: 17909032]

17. Schadendorf D, Jurgovsky K, Kohlmus CM, Czarnetzki BM. Glutathione and related enzymes in tumor progression and metastases of human melanoma. J Invest Dermatol. 1995; 105:109–12. [PubMed: 7615963]
18. Awasthi YC, Sharma R, Sharma A, et al. Self-regulatory role of 4-hydroxynonenal in signaling for stress-induced programmed cell death. Free Radic Biol Med. 2008; 45:111–8. [PubMed: 18456001]
19. Singhal SS, Saxena M, Ahmad H, Awasthi S, Haque AK, Awasthi YC. Glutathione S-transferases of human lung: Characterization and evaluation of the protective role of the alpha-class isozymes against lipid peroxidation. Arch Biochem Biophys. 1992; 299:232–41. [PubMed: 1444461]
20. Woodard J, Platanias LC. AMP-activated kinase (AMPK)-generated signals in malignant melanoma cell growth and survival. Biochem Biophys Res Commun. 2010; 398:135–9. [PubMed: 20599746]
21. Meier F, Schittek B, Busch S, et al. The RAS/RAF/MEK/ERK and PI3K/AKT signaling pathways present molecular targets for the effective treatment of advanced melanoma. Front Biosci. 2005; 10:2986–3001. [PubMed: 15970553]
22. Chu YW, Seftor EA, Romer LH, Hendrix MJ. Experimental coexpression of vimentin and keratin intermediate filaments in human melanoma cells augments motility. Am J Pathol. 1996; 148:63–9. [PubMed: 8546227]
23. McCarthy JB, Furcht LT. Laminin and fibronectin promote the haptotactic migration of B16 mouse melanoma cells *in vitro*. J Cell Biol. 1984; 98:1474–80. [PubMed: 6715409]
24. Yin F, Giuliano AE, Law RE, Van Herle AJ. Apigenin inhibits growth and induces G2/M arrest by modulating cyclin-CDK regulators and ERK MAP kinase activation in breast carcinoma cells. Anticancer Res. 2001; 21:413–20. [PubMed: 11299771]
25. Woo KJ, Lee TJ, Bae JH, et al. Thimerosal induces apoptosis and G2/M phase arrest in human leukemia cells. Mol Carcinog. 2006; 45:657–66. [PubMed: 16649253]
26. Tsao H, Atkins MB, Sober AJ. Management of cutaneous melanoma. N Engl J Med. 2004; 351:998–1012. [PubMed: 15342808]
27. Phan GQ, Attia P, Steinberg SM, White DE, Rosenberg SA. Factors associated with response to high dose interleukin-2 in patients with metastatic melanoma. J Clin Oncol. 2001; 19:3477–82. [PubMed: 11481353]
28. Ribas A, Hersey P, Middleton MR, et al. New challenges in endpoints for drug development in advanced melanoma. Clin Cancer Res. 2012; 18:336–41. [PubMed: 22142824]
29. Yadav S, Zajac E, Singhal SS, Awasthi S. Linking stress-signaling, glutathione metabolism, signaling pathways and xenobiotic transporters. Cancer Metastasis Rev. 2007; 26:59–69. [PubMed: 17260165]
30. Proctor RA, Dalal SC, Kahl B, Brar D, Peters G, Nichols WW. Two diarylurea electron transport inhibitors reduce Staphylococcus aureus hemolytic activity and protect cultured endothelial cells from lysis. Antimicrob Agents Chemother. 2002; 46:2333–6. [PubMed: 12121901]
31. Bedrosian I, Faries MB, Guerry D, et al. Incidence of sentinel node metastasis in patients with thin primary melanoma (≤ or 0 1 mm) with vertical growth phase. Ann Surg Oncol. 2000; 7:262–7. [PubMed: 10819365]
32. Davies MA, Stemke-Hale K, Lin E, et al. Integrated molecular and clinical analysis of AKT activation in metastatic melanoma. Clin Cancer Res. 2009; 15:7538–46. [PubMed: 19996208]
33. Govindarajan B, Sligh JE, Vincent BJ, et al. Over-expression of akt converts radial growth melanoma to vertical growth melanoma. J Clin Invest. 2007; 117:719–29. [PubMed: 17318262]
34. Jiang CC, Yang F, Thorne RF, Zhu BK, Hersey P, Zhang XD. Human melanoma cells under endoplasmic reticulum stress acquire resistance to microtubule-targeting drugs through XBP-1-mediated activation of akt. Neoplasia. 2009; 11:436–47. [PubMed: 19412428]
35. Gopal YN, Deng W, Woodman SE, et al. Basal and treatment-induced activation of AKT mediates resistance to cell death by AZD6244 (ARRY-142886) in braf-mutant human cutaneous melanoma cells. Cancer Res. 2010; 70:8736–47. [PubMed: 20959481]
36. Chawla-Sarkar M, Bae SI, Reu FJ, Jacobs BS, Lindner DJ, Borden EC. Down-regulation of bcl-2, FLIP or IAPs (XIAP and survivin) by siRNAs sensitizes resistant melanoma cells to Apo2L/TRAIL-induced apoptosis. Cell Death Differ. 2004; 11:915–23. [PubMed: 15118763]

37. Plettenberg A, Ballaun C, Pammer J, et al. Human melanocytes and melanoma cells constitutively express the bcl-2 proto-oncogene in situ and in cell culture. Am J Pathol. 1995; 146:651–9. [PubMed: 7887447]

38. Anvekar RA, Asciolla JJ, Missert DJ, Chipuk JE. Born to be alive: A role for the BCL-2 family in melanoma tumor cell survival, apoptosis, and treatment. Front Oncol. 2011; 1:00034.

39. Yamamura K, Kamada S, Ito S, Nakagawa K, Ichihashi M, Tsujimoto Y. Accelerated disappearance of melanocytes in bcl-2-deficient mice. Cancer Res. 1996; 56:3546–50. [PubMed: 8758925]

40. Dai DL, Wang Y, Liu M, Martinka M, Li G. Bim expression is reduced in human cutaneous melanomas. J Invest Dermatol. 2008; 128:403–7. [PubMed: 17637819]

41. Villa R, Zaffaroni N, Bearzatto A, Costa A, Sichirollo A, Silvestrini R. Effect of ionizing radiation on cell-cycle progression and cyclin B1 expression in human melanoma cells. Int J Cancer. 1996; 66:104–9. [PubMed: 8608951]

42. Nagaprashantha LD, Vatsyayan R, Lelsani PC, Awasthi S, Singhal SS. The sensors and regulators of cell-matrix surveillance in anoikis resistance of tumors. Int J Cancer. 2011; 128:743–52. [PubMed: 20949625]

43. Bumol TF, Reisfeld RA. Biosynthesis and secretion of fibronectin in human melanoma cells. J Cell Biochem. 1983; 21:129–40. [PubMed: 6411743]

44. Li M, Zhang B, Sun B, et al. A novel function for vimentin: The potential biomarker for predicting melanoma hematogenous metastasis. J Exp Clin Cancer Res. 2010; 29:109. [PubMed: 20701774]

45. Hardie DG. Minireview: The AMP-activated protein kinase cascade: The key sensor of cellular energy status. Endocrinology. 2003; 144:5179–83. [PubMed: 12960015]

46. Zheng B, Jeong JH, Asara JM, et al. Oncogenic BRAF negatively regulates the tumor suppressor LKB1 to promote melanoma cell proliferation. Mol Cell. 2009; 33:237–47. [PubMed: 19187764]

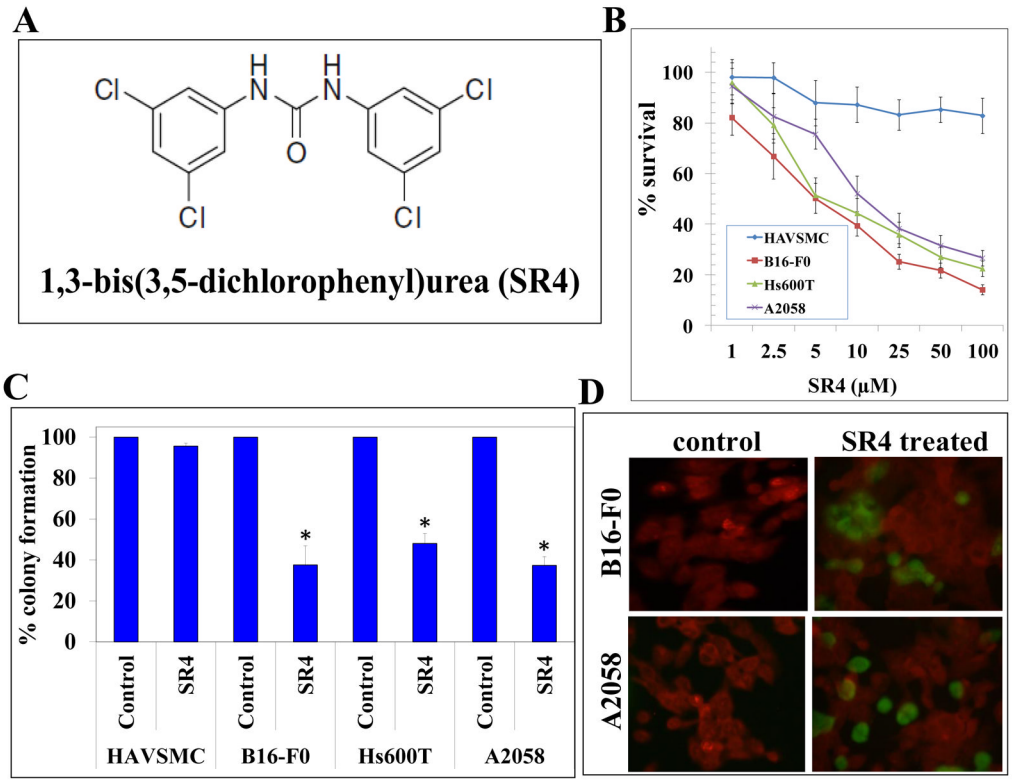

Figure 1. Anti-proliferative and pro-apoptotic effects of SR4 in Melanoma

The chemical structure of 1,3-bis(3,5-dichlorophenyl)urea compound also called COH-SR4 (**panel A**). Drug sensitivity assays were performed by MTT assay using SR4 at 96 h post-treatment to determine IC_{50}. Values are presented as mean ± standard deviation from two separate determinations with eight replicates each (n= 16) (**panel B**). Colony-forming assay was performed and the colonies were counted using Innotech Alpha Imager HP as detailed in Materials and Methods. * $p < 0.001$ compared with control (n=3, **panel C**). For TUNEL apoptosis assay, cells were grown on coverslips and treated with 10 μM SR4 for 24 h. TUNEL assay was performed using Promega fluorescence detection kit and examined using Zeiss LSM 510 META laser scanning fluorescence microscope with filters 520 and 620 nm. Photographs taken at identical exposure at × 400 magnification are presented. Apoptotic cells showed green fluorescence (**panel D**).

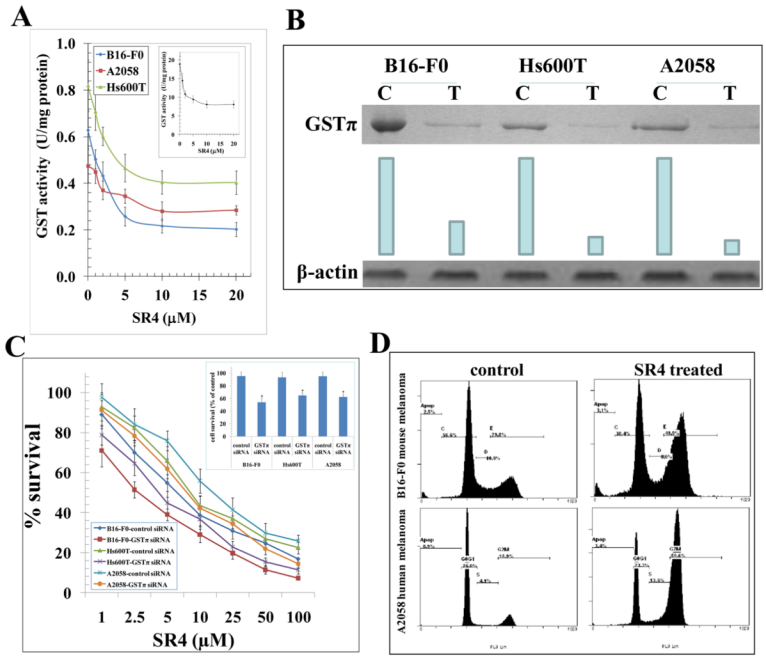

Figure 2. Effect of SR4 on cell cycle progression in melanoma

GST activity towards 1-chloro 2,4-dinitro benzene (CDNB) and its inhibition by SR4 was performed in 28000g crude supernatant prepared from B16-F0, Hs600T and A2058 cells. Human liver purified GST was used as a control (**inset**). The inhibitory effect of SR4 on GST was studied at a fixed concentration of GSH and CDNB (1 mM each) and varying concentrations of inhibitor. The enzymes were pre-incubated with the inhibitor for 5 min at 37 °C prior to the addition of the substrates (**panel A**). **Depletion of GSTπ by siRNA and its effects on cell survival by MTT assay:** GSTπ siRNA or a scrambled control was transfected into melanoma cell lines using Lipofectamine 2000 (Invitrogen). After knock-down of GSTπ by siRNA, the level of GSTπ was detected by Western blot analyses. Membranes were stripped and reprobed for β-actin as a loading control. Results were quantified by scanning densitometry: **C**, control siRNA; **T**, GSTπ siRNA (**panel B**). MTT assay in GSTπ siRNA transfected cells were performed 96 h after SR4 treatment. The values are presented as mean ± SD from two separate determinations with eight replicates each (n = 16) (**panel C**). GSTπ-depletion itself caused decreased in cell growth(**panel C inset**), * $p<0.01$ compared to control. Inhibitory effect of SR4 on cell cycle distribution was determined by fluorescence activated cell sorting (FACS) analysis (**panel D**). The experiment was repeated three times and similar results were obtained.

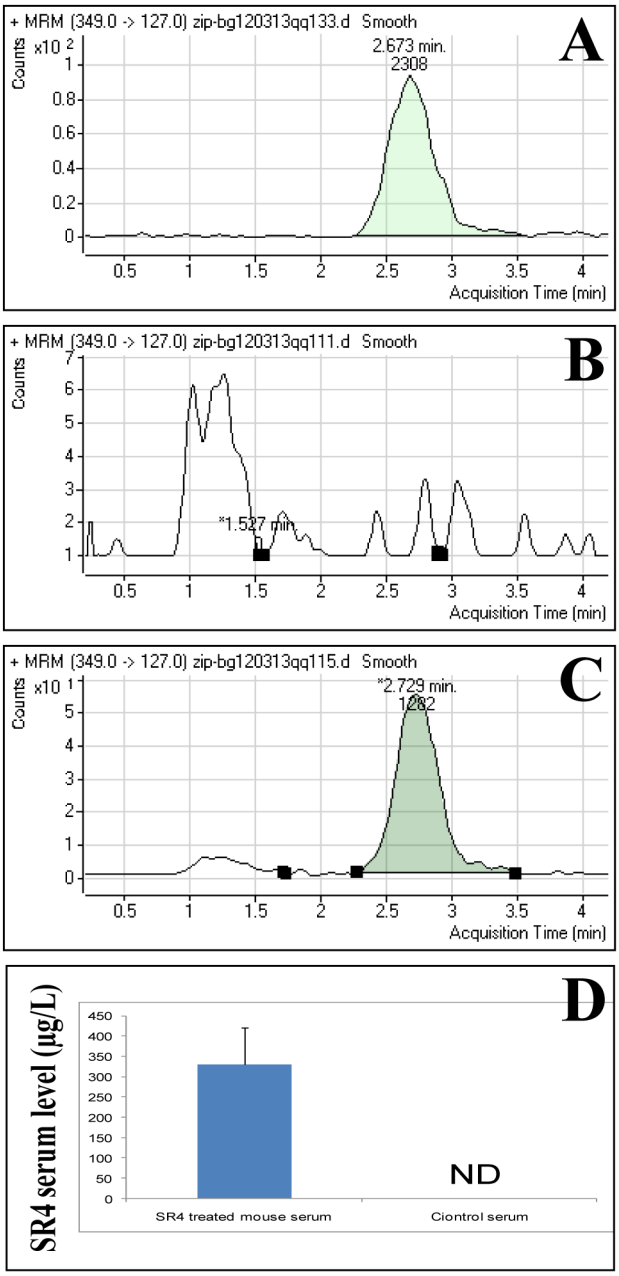

Figure 3. Measurement of serum levels of SR4

The serum levels of SR4 in control and SR4 treated mice was examined by LC-MS/MS analyses. The C57 B mice were treated with 0.1 mg/mice (4 mg/kg b.w.) of SR4 on alternate day by oral gavage for 8 weeks. On the final day of treatment blood was collected within 2 h of final dosage. The samples were processed and analyzed for serum levels of SR4 as described in the methods section. The panels represent multiple reaction monitoring (MRM) mode chromatograms of 6D-SR4 standard 5 pg/uL (**panel A**), control serum (**panel B**) and SR4 treated mice serum (**panel C**). The bar diagram represents the quantification (mean ± SD) of SR4 in mice serum (n = 3); ND, not detectable (**panel D**).

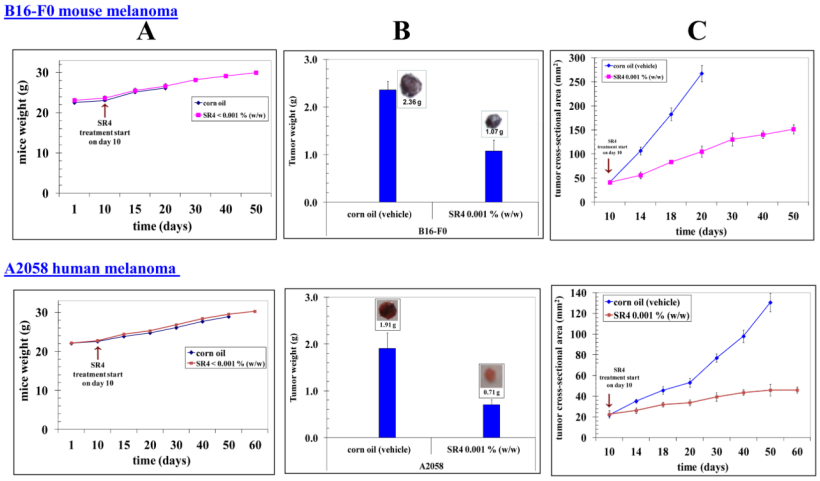

Figure 4. Effect of oral administration of SR4 on melanoma progression in mice

The C57B mice and Hsd: Athymic nude nu/nu mice were obtained from Harlan, Indianapolis, IN. In each model, ten 10-weeks-old mice were divided into two groups of 5 animals (treated with corn oil (vehicle), and SR4 compound 4 mg / kg b.w.). All animals were injected with 2×10^6 melanoma cells suspensions in 100 μl of PBS, subcutaneously into one flank of each mouse. Treatment was started 10 days after the implantation to see palpable tumor growth. Treatment consisted of 0.1 mg of SR4/mice in 200 μl corn oil by oral gavage alternate day. Control groups were treated with 200 μl corn oil by oral gavage alternate day. Animals were examined daily for signs of tumor growth and body weights were recorded (**panel A**). Photographs of animals were taken at day 1, day 10, day 14, day 18, day 20, day 30, day 40, and day 60 after subcutaneous injection, are shown for all groups (supplementary Figures 2 and 3). Weights and photographs of tumors were also taken at day 20 (for syngeneic model), and at day 51 (for xenograft model). Photographs of tumors were also taken at day 20 (for syngeneic model), and at day 51 (for xenograft model) (**panel B**). Tumors were measured in two dimensions using calipers and time-course analysis of tumor regression was performed during the study (**panel C**).

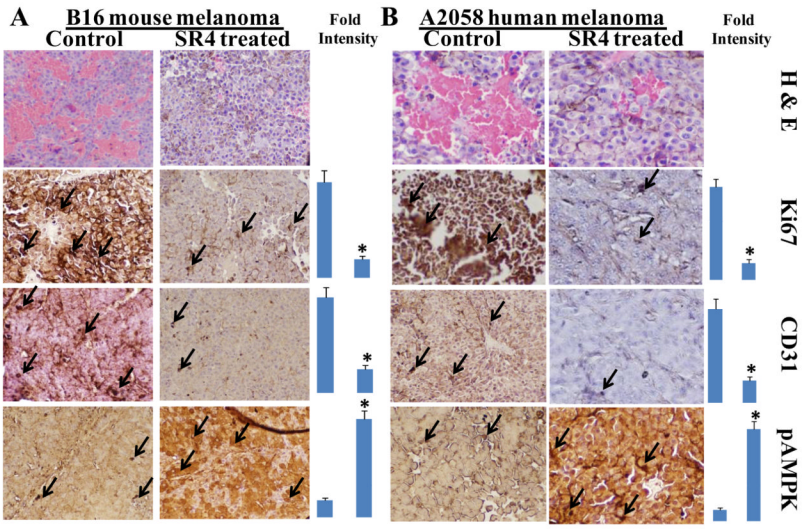

Figure 5. Histopathologic analyses of tumor sections after SR4 treatment

Control and SR4 treated B16-F0 and A2058 melanoma bearing mice tumor sections were used for histopathologic analyses. Immuno-histochemistry analyses for Ki-67, CD31, and pAMPK expression from tumors in mice of control and SR4-treated groups. Statistical significance of difference was determined by two-tailed Student's t test. $p < 0.001$, SR4-treated compared with control. Immuno-reactivity is evident as a dark brown stain, whereas non-reactive areas display only the background color. Sections were counterstained with Hematoxylin (blue). Percent staining was determined by measuring positive immuno-reactivity per unit area. Arrows represent the area for positive staining for an antigen (**panel A-** Histopathology of resected B16-F0 syngeneic mouse melanoma tumors; **panel B-** Histopathology of resected A2058 human melanoma tumors). The intensity of antigen staining was quantified by digital image analysis. Bars represent mean ± S.E. (n = 5); * $p<0.001$ compared with control

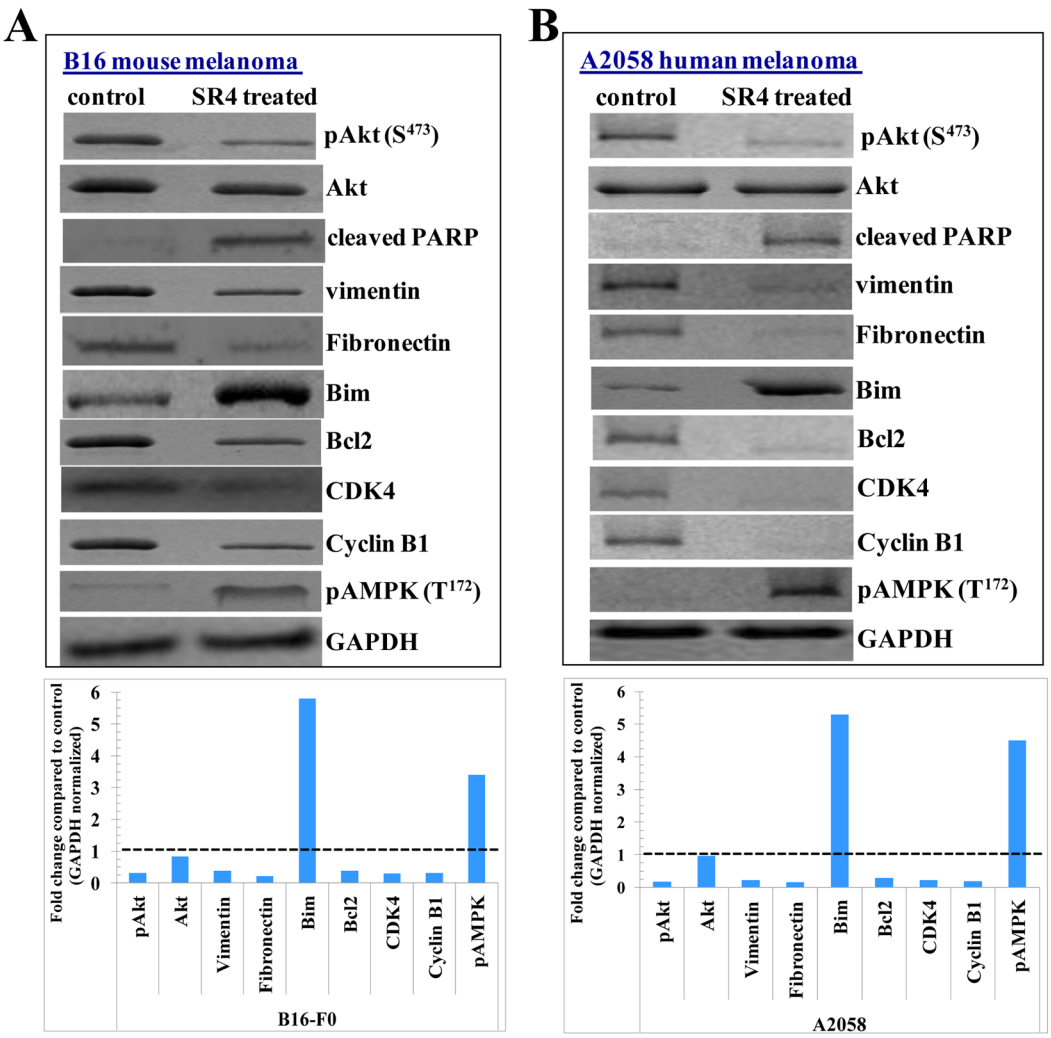

Figure 6. Effect of SR4 on signaling proteins *in vivo* models of melanoma

Western-blot analyses of signaling proteins in tumor tissue lysates in control and SR4 treated experimental groups (**panel A-** Western blot of lysates from resected B16-F0 syngeneic mouse melanoma tumors from C57 B mice; **panel B-** Western blot of resected A2058 human melanoma tumors from *nu/nu* nude mice xenograft model). The bar diagrams represent the fold change in the levels of proteins as compared to controls as determined by densitometry. Dotted line represents no significant change as observed with control.